CRITICAL REVIEW OF NUMERICAL STRESS ANALYSIS TOOLS FOR DEEP COAL LONGWALL PANELS UNDER STRONG STRATA

M. K. Larson, NIOSH, Spokane, WA
J. K. Whyatt, NIOSH, Spokane, WA

ABSTRACT

Proper employment of numerical stress analysis design tools is based on the demonstrated ability of a model to capture key elements of the geologic site model and accurately simulate how these elements interact with a mine design. While these tools have progressed markedly, they are, at heart, a gross simplification of the abundant complexity of a natural setting and its response to mining. A generic deep longwall site model was developed that includes aspects of the geology of deep coal mines in the Wasatch Plateau and Book Cliffs coal fields of Utah. The site model contains a set of common features and observations of how these features typically respond to mining. This site model was the basis for evaluating use of empirical, boundary element and volume element stress analysis tools to analyze the distribution of stress around a deep longwall panel. More specifically, this evaluation examined shifting of stress to panel abutments and gob, distribution of stress in the abutment, and deformation and failure of bridging strata. Measurements of abutment stress changes at two sites in the Wasatch Plateau region were used to illustrate model calibration. Overall, these comparisons highlight the considerable differences between methods. Volume element tools can incorporate considerable detail and have fewer underlying assumptions, but this detail carries a considerable computational cost. Boundary element tools are much more efficient. But this efficiency also comes at a cost of added assumptions. These assumptions were challenged by the presence of a strong sandstone unit in the overburden, leading to boundary element results that depart significantly from volume element results. Empirical rules are the simplest, but are even more burdened by assumptions, many of which are implicit in underlying cases. Insight into the nature and impacts of underlying assumptions in each method is essential to proper use of results in mine design.

Disclaimer: The findings and conclusions in this report are those of the authors and do not necessarily represent the views of the National Institute for Occupational Safety and Health

INTRODUCTION

The application of numerical stress analysis tools to ground control and mine design holds great promise but can also provide an unwarranted confidence in results. It is important that both practitioners and those who review and implement design based on numerical models have insight into the strengths and weaknesses of these tools. This report describes a study undertaken by the National Institute for Occupational Safety and Health (NIOSH) to more fully appreciate the application of numerical models in support of research on dynamic failure (bumps and bounces) in deep western coal mines.

The study is based on a simplified generic site model with features typical of the Book Cliffs and Wasatch Plateau coal fields of Utah. This model includes a simplified stratigraphic column, estimates of relative properties of various strata, and most importantly, observations of typical large-scale response to mining of a single, isolated panel. In this study, the quantitative values of specific material properties are not as important as the ratios between values of the same property among strata members. These ratios can be greater in the Utah coal region than in the rest of the U.S [2]. Stress analyses are conducted with an empirical method, a boundary element program (LaModel) [16] and a volume element program (FLAC) [20]. Selected model results are compared, including (1) shifting of stress to panel abutments and gob, (2) distribution of stress in the abutment, and (3) deformation and failure of bridging strata. Stress measurements from two panels are used to demonstrate calibration of these models to specific sites. Subsidence and multiple-panel effects are also of interest but are not addressed in this paper.

MODELING GOAL

An important first step in developing a geomechanical model is careful consideration and definition of goals for the modeling exercise. In this case, the goal is to compare performance of empirical, boundary element and volume element analysis methods for a site model typical of deep western coal mines—that is, a coal mine under an interval of strong, massive strata within softer, weaker strata. A simple case is chosen--mining of a single panel surrounded by solid abutments (or very large barrier pillars). The case is further simplified by considering only a two-dimensional cross section located near the middle of a long panel. Only subcritical panels are considered in order to study stress transfer to abutments that might result in bump-prone conditions.

Mining of a panel undercuts strata, causing caving and redistribution of vertical and horizontal stress. Some combination of bulking of caved material and subsidence of overburden usually result, allowing the caved material (gob) to support some portion of the weight of overlying strata. The remaining weight is carried to panel abutments by an arch or bridge in the overlying strata. Stress in the abutments is increased by this added weight, an increase often described as the mining-induced stress. The magnitude and distribution of mining-induced stress can be estimated based on underground observations, empirical relationships, or models using a variety of numerical methods. Whatever the method, three key quantities are estimated. These are (1) the proportion of load transmitted to the abutments, (2) the distance that mining-induced stress is transmitted into the abutment[1], and (3) the magnitude and location of peak stress in the abutment rib. These factors are illustrated in figure 1.

OBSERVATIONS

Panel mining methods, both pillar and longwall, rely on caving to limit stress transfer to neighboring pillars and abutments. The critical width is the span at which arching or bridging has failed to the surface and maximum subsidence obtained. It can be described as the panel width, with reference to figure 2, when the lines extending upward from each rib at angle β intersect at the surface; it represents the vertical section geometry where caving and abutment loading conditions that form the boundary between subcritical and super-critical conditions. Crushing of yield pillars, where they are used, more gradually transfers stress across the entries to the solid abutment. Thus, the effective span in these cases includes the entries and can span multiple panels if they are separated only by yield pillars. Indeed, due to the greater mining depth, the critical width in deep western coal mines is often several panels. For example, the critical width at the Deer Creek mine occurred with mining of the third panel [2].

[1] In this report, the distance from the gob that mining induced stress is transferred onto the coal seam is referred to as the stress transfer distance.

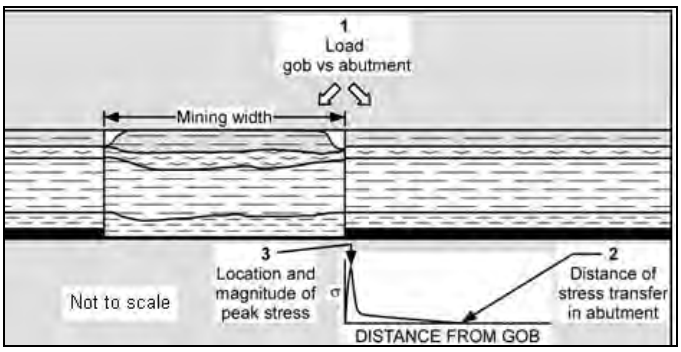

Figure 1. Vertical cross section across the width of a panel showing important concepts of stress redistribution resulting from excavation of a single panel.

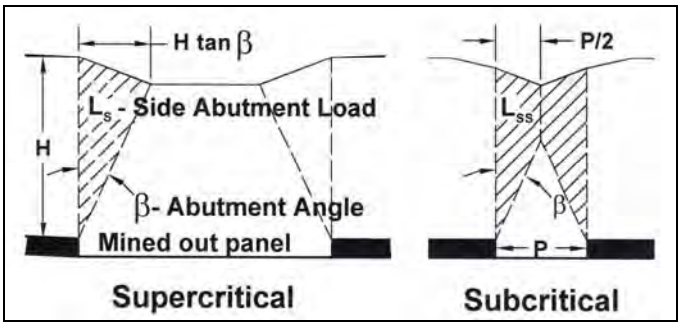

Figure 2. Vertical cross section across the width of mined panels showing geometry of supercritical (left) and subcritical (right) panels after Heasley [17]. The subcritical geometry is used by Mark [31] in ALPS.

Maleki [30] reviewed relationships between minimum pressure arch width and depth of overburden, including the Holland equation [19] and estimates based on his own measurements of gob stress. These are plotted in Figure 3 against

$$2H\tan(21°),$$

an empirical relationship used in ALPS (Analysis of Longwall Pillar Stability [31], an empirical method of assessing the stability of gate road pillars in longwall mining). These criteria generate a wide range of arch widths, particularly at depth.

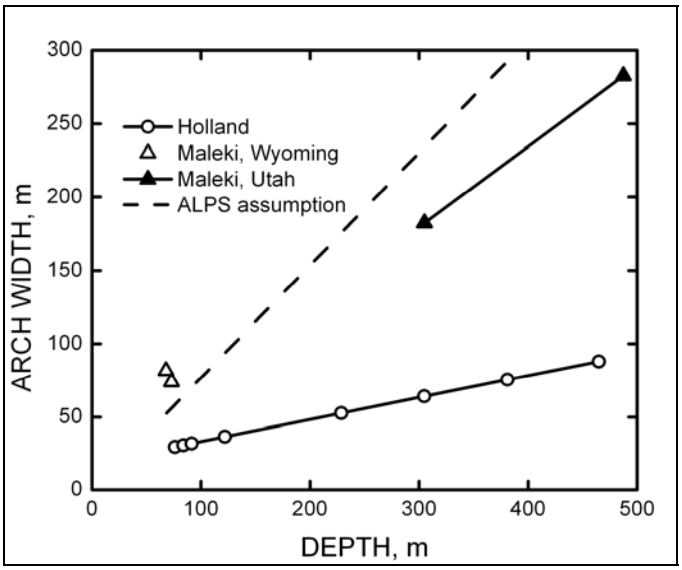

Figure 3. Maleki's pressure arch graph [30] with ALPS assumption curve added.

The weight of bridging strata and strata that cantilevers over the cave is shifted to pillars and abutments surrounding the panel. Since the maximum bending stress in beams with clamped ends are generally greater than in cantilevers [6;39], strong, thick strata beams often cave in large sections that may span the width of the panel. Completion of caving can substantially reduce the amount of weight that is shifted to the abutment.

In observations, the full extent of stress transfer is not detectable. The distance at which neighboring openings are impacted by shifting of stress is a practical quantity, but that quantity may vary according to site conditions. Therefore, for purposes of comparison, the distance at which the calculated vertical stress on the seam returns to 50% of the premining stress will be used as a measure. This level is arbitrary, but is equivalent to a 50% increase in overburden, an increase that will certainly be evident in driving of an entry. Observations in the literature refer to a "detectable" increase in stress, when determining as the stress transfer distance [13].

Observations of stress transfer distances are often remarked upon in discussions of ground behavior in deep western coal mines. Generally, distances are considered notable because of their long length. These observations also hint at the importance of anticipating these distances. These observations include:

- DeMarco et al. [11] discuss western U.S. longwall operations and report that units of strong, competent strata transfer "considerable abutment loads over relatively large distances."
- Koehler [23] reported stresses overriding a 46-m- (150-ft-) wide barrier pillar to cause bump events at the Sunnyside No. 1 mine (also discussed by Chen et al. [9]). The mine was under 610 m (2000 ft) of overburden with 55-m-thick (180-ft-thick) sandstone about 46 m (150 ft) above the coal seam.
- Barron [5] described stress transferring from the longwall face in a Book Cliffs mine in strong strata. Stresses induced by a 150-m- (500-ft-) wide face caused tailgate pillars to "explode without warning" 90 to 150 m (300 to 500 ft) outby the face.
- Gilbride and Hardy [12] found barrier pillars "as wide as 120 m (390 ft) or more may be necessary for pillar stability and abutment protection when depths reach 900 m (3000 ft) or more."
- Maleki [29] found good performance for a 150-m-wide (490-ft-wide) barrier in the Rock Canyon and Gilson seams with 580 m [1900 ft] maximum overburden .
- Goodrich et al. [13] found load transfer distances greater than 230 m (750 ft) at the Deer Creek Mine. A pillar burst and other stress-induced ground conditions were apparent in a developed gate road as mining passed in the previous panel, with a full panel of intact coal seam serving as a barrier. Stress measurements suggested a 13% increase in stress was transferred over the panel.

EMPIRICAL METHOD

Empirical methods have been proposed to estimate the redistribution of stress, including a scheme that has been integrated into the empirical design tools ALPS and ARMPS [31;33]. This approach begins with a simple estimate of the load transfer distance using the equation of Peng and Chiang [40]:

$$D = 9.3\sqrt{H}, \quad (1)$$

where: D = distance from the gob (ft), and
H = depth of overburden (ft).

That is, the influence of a panel on stress conditions in neighboring areas disappears entirely at a distance D. The additional load carried within this distance in each abutment of a subcritical panel can be calculated from a simple geometric model of arching overburden (figure 2). The angle β defines a triangular "arch" that

bounds caving. The weight of caved material is transmitted through the gob to the panel floor. When $H \tan \beta$ reaches half the panel width, the arch reaches the surface and abutment loading reaches its maximum. This geometry is called the critical span.

Mark [32] determined β at six sites in four mines in the eastern U.S. coal fields. He [31] identified three of the mines as the Kitt Mine (Lower Kittanning Seam), the Lynch Mine (Harlan Seam), and the Quarto #4 Mine (Pittsburgh No. 8 Seam). He found values of β ranging from 10.7° to 25.2°. He concluded that a value of β = 21° would yield appropriately conservative estimates of side abutment load for longwall pillar design for these and similar cases. Significantly higher values have been reported. For example, a similar geometric model applied to subsidence at the Deer Creek Mine in the Wasatch Plateau region of Utah (figure 4), showed a critical span of 1.6*H*, or β = 38.6° [3]. The National Coal Board uses a similarly high value of 35° [35]. These results indicate that 21° may not be conservative at sites that differ markedly from those studied by Mark. In this report, β = 21°, the recommended value for ALPS method, was used to calculate abutment stresses.

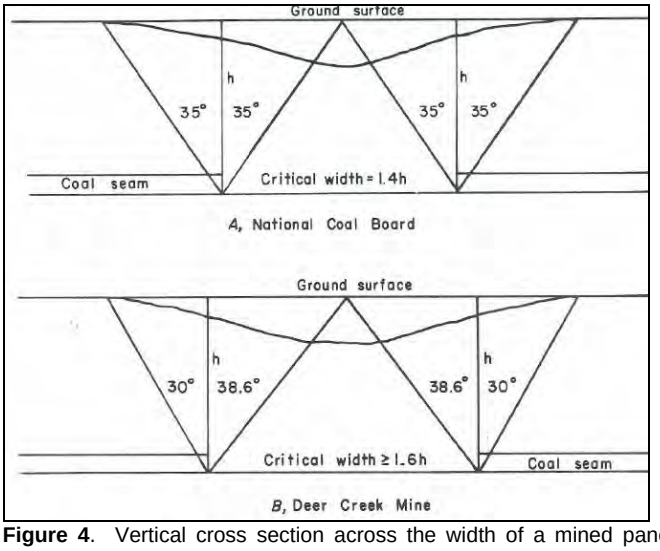

Figure 4. Vertical cross section across the width of a mined panel showing critical mining widths from the National Coal Board (A) and Deer Creek Mine (B); after Allgaier [3].

For this empirical model of a subcritical panel, the additional load carried in each abutment is

$$L_{ss} = \left[\frac{HP}{2} - \frac{P^2}{8\tan\beta}\right]\gamma, \quad (2)$$

where L_{ss} = the total subcritical panel abutment load (from figure 2),

P = panel width, and
γ = density of the overburden.

Mark [32] also proposed a function to describe the distribution of added stress in the abutment. This function is:

$$\sigma_a = \left(\frac{3L_{ss}}{D^3}\right)(D-x)^2, \quad (3)$$

where σ_a = the additional vertical stress at point in the abutment caused by mining, and

x = distance of that point from the abutment rib.

For supercritical panels, L_s (figure 2) is substituted for L_{ss} in equation (3), where

$$L_s = H^2(\tan\beta)\left(\frac{\gamma}{2}\right). \quad (4)$$

Since the premining vertical stress on the seam is, on average

$$\sigma_{vo} = H\gamma, \quad (5)$$

equation (3) can be normalized with respect to premining vertical stress for the subcritical case as follows:

$$\frac{\sigma_a}{\sigma_{vo}} = \frac{3\left[\frac{HP}{2} - \frac{P^2}{8\tan\beta}\right]}{(9.3)^3 H^{\frac{5}{2}}}\left(9.3\sqrt{H} - x\right)^2. \quad (6)$$

Figure 5 shows the effects of varying overburden depth (H) and panel width (P) with constant cave angle (β). Panel width affects normalized peak stress, whereas overburden depth affects the stress transfer distance (only).

The location of a 50% increase in overburden stress is given by

$$x_{50\%\ premining\ stress} = 9.3\sqrt{H} - \sqrt{\frac{0.5(9.3)^3 H^{\frac{5}{2}}}{3\left[\frac{HP}{2} - \frac{P^2}{8\tan\beta}\right]}}. \quad (7)$$

In figure 5, the location of this point along each curve is indicated by its intersection with the dotted, horizontal line.

GENERIC SITE MODEL

A site model is the starting point for any numerical modeling study. The site model includes key elements of the geologic setting, mining plan, and mechanical properties. In this case, a simple generic site model was developed from a review of literature describing geology and geomechanical response of geology to longwall mining in the Wasatch Plateau and Book Cliffs coal fields of Utah. These regions are characterized by the presence of strong, thick sandstone strata, a characteristic that strongly contrasts with overburden in many other U.S. coal fields. Agapito et al. [2] describe these strata as "thick, competent overburden strata that tend to bridge and interlock" and "very competent and strong immediate roof and floor sandstone/siltstone strata." This site model is not required, or considered, for empirical calculations of the previous section. Those results implicitly assume a site model that is similar to a case or cases underlying the empirical method. Significant departures from conditions in these underlying cases in application can compromise results. In other words, the empirical method has its own site model.

Generic Model Description

The generic site model was designed to be a simple but representative geologic column typical of deep western coal mines. Any massive stratum with bridging potential is labeled "sandstone" while weaker strata are labeled "shale" or "soft shale" (including mudstones, siltstones and even thinly bedded sandstone). Typically, floor and overburden include strong, stiff and massive sandstone members. The immediate roof can be sandstone or shale. An idealized geologic column was formulated with a sandstone floor overlain by coal, an immediate roof of shale, a sandstone layer and then soft shale to the surface (figure 6). Panel width was set at 240 m (800 ft). A 610 m (2000 ft) thick sandstone floor was defined in volume-element models (the floor of a boundary element model is infinitely thick).

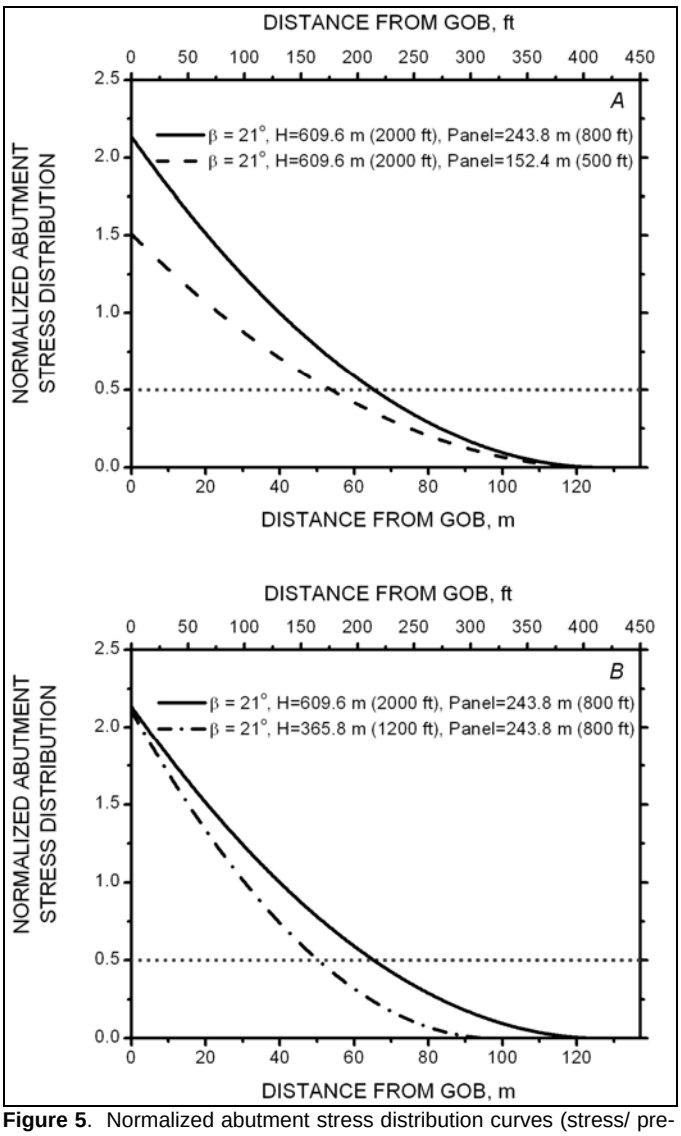

Figure 5. Normalized abutment stress distribution curves (stress/ pre-mining stress - 1). A, Variation of panel width; and B, variation of overburden thickness. The closely dotted line near the bottom of each graph indicates a 50% increase in vertical stress over premining stress.

Properties set for each unit are listed in Table 1 (see Appendix). These properties were based on reports of laboratory properties on samples taken from the Book Cliffs/Wasatch Plateau area and properties used in models of specific sites in the region [1;14;21;25;27-29;38]. The sandstone Young's modulus was selected to be in the upper part of the reported range to emphasize the contrast with shale. The tensile strength of the immediate roof shale was chosen somewhat high to avoid numerical difficulties caused by localization of severely deformed zones resulting from very high stress concentrations in the volume element model. A cave and gob model was employed in some models to separately account for shale roof failure in tension.

The sensitivity of model results to variations of thickness members of this column was explored by using three thicknesses of immediate roof shale (0, 3.0, and 15 m [0, 10, and 50 ft]) and four thicknesses of roof sandstone (3.0, 15, 61, and 150 m [10, 50, 200, and 500 ft]). For convenience in generating the volume-element grid, a joint interface was placed between each member. These interfaces were numerically "glued" to prevent slip. A ubiquitous joint model was used to allow slip and separation along shale bedding planes.

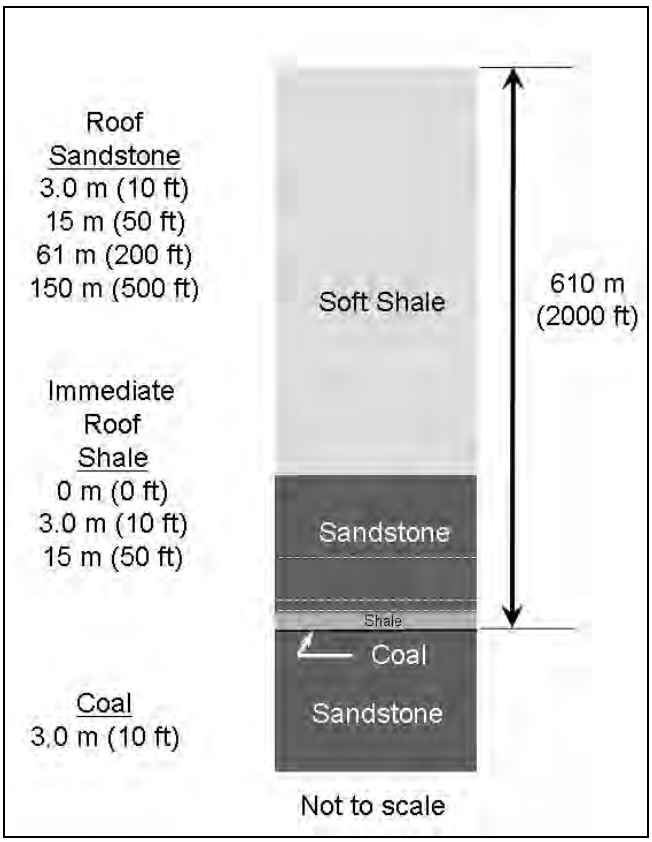

Figure 6. Geologic column of generic model with indicated thickness of members used in models.

MODEL DEVELOPMENT

Implementation in a Volume Element Model

The volume element approach discretizes individual volumes of the rock mass, allowing for more detail in representing geology and mine geometry, and more complex constitutive behavior. This ability comes at the cost of much greater computational requirements. To compensate, many analyses consider only a two-dimensional section through the mine. The volume element approach is used by finite element and finite difference programs, in this case the program FLAC2D [20]. Three-dimensional models can also be run but are usually limited to a single panel because of computational limitations. Some of the most comprehensive three-dimensional modeling studies of coal longwall panels that have been published have addressed Australian coal mines (e.g., [4;22]). Kelly's [22] models project the location and type of fracturing around a panel. Badr et al. [4] conducted a detailed study of yield pillar design for typical western longwall conditions.

The extent of caving, where modeled, was assumed to propagate through the immediate roof shale to a bridging sandstone layer. This layer could then be tested for failure by implementation of a failure criterion. The gob roof as viewed in vertical section across the width of the mined panel was initially assumed to form an ellipse, whose horizontal axis was 50% larger than the thickness of the shale. However, preliminary model results showed shale above the curved gob line in the first model always failed. Therefore, caving of all immediate roof shale above the extracted portion of the seam is assumed. Stresses were initialized according to gravity loading, and the sides and bottom of the model were "rollered" (displacement fixed in the direction normal to the surface) in FLAC, creating a lithostatic in-situ stress field.

Gob stress was calculated and applied as nodal forces on the roof and floor of the extracted volume. The gob stress-closure equation followed the best-fit relation of Pappas and Mark [37] for shale to Salamon's equation [42]. Nonlinear models lacking gob proved

sensitive to the sudden application of loading, resulting in overestimates of plastic strain and yield. In this case, pre-excavation forces were applied to the gob roof and floor and incrementally decreased.

Implementation in a Boundary Element Model

The boundary element approach reduces the computational intensity of problems to manageable levels by reducing the problem by one dimension. This is accomplished by modeling the coal seam as a crack in an infinite elastic body (e.g., [15;43;46;47]). Depending on the formulation, the elastic body can be isotropic or anisotropic, or can be divided into a series of uniform elastic layers between frictionless interfaces. This last formulation is used by LaModel [16], the boundary element program used in this study. It has proven particularly useful in simulating the behavior of weak and highly stratified overburden found in many U.S. coalfields. A great strength of the boundary element method is its ability to fully consider the geometry of a mine, including mining of multiple seams, in relatively quick runs (compared to volume element methods). LaModel is one of the fastest of these codes; largely because it limits calculations to vertical loading (horizontal stresses are neither input nor calculated). Guidelines published by Heasley [18] for model development with LaModel were followed except where explicitly noted.

One of these guidelines provides assistance in selecting layer thickness from the equation:

$$t = \frac{2E_s\sqrt{12\left(1-\upsilon^2\right)}}{Eh}\left(\frac{5\sqrt{H}-d}{\ln(0.1)}\right)^2, \quad (8)$$

where E = elastic modulus of the overburden,

υ = Poisson's ratio of the overburden,
E_s = elastic modulus of the seam,
h = seam thickness,
d = extent of the coal yielding at the gob edge, and
H = seam depth.

One interesting feature of this equation is that the product of elastic modulus and thickness is a constant. That is:

$$tE = \text{constant}. \quad (9)$$

Heasley's calibration guidelines [18] produce values for E and t, but an equivalent result can be achieved by varying E and t according to equation 9.

Often it is beneficial to use multiple modeling methods to study a problem. For example, one may wish to compare LaModel results with those from a model with a massive elastic overburden. This might be another boundary element program like MULSIM/NL (multiple seams, nonlinear) [46;47] or a simple FLAC model. In such a case, it is important to realize that properties that seem similar are not always equivalent. Overburden elastic modulus is a case in point, especially for LaModel, because of its dependence on lamination thickness. In fact, MSHA [34], based on Heasley's formulation [15], showed how any combination of homogeneous and laminated moduli can be made equivalent for a particular panel width by choosing the lamination thickness (t), according to:

$$t = \sqrt{\frac{3}{4}}\frac{E_{homogeneous}}{E_{laminated}}\frac{L}{\sqrt{1-\upsilon^2}}, \quad (10)$$

where t = lamination thickness,

$E_{homogeneous}$ = Young's modulus of a homogeneous overburden,

$E_{laminated}$ = Young's modulus of a laminated overburden,

L = half width of the longwall panel, and

υ = rock mass Poisson's ratio.

Note that this relationship depends on panel width as well as material properties. Put another way, if panel behavior is well-described by an overburden mass modulus, the panel width must be considered when translating to a laminated layer modulus for LaModel. Equation 10 can be reconfigured to find the invariant overburden product (equation 9) for LaModel that is equivalent to a given mass modulus as follows:

$$E_{laminated}\ t = E_{homogeneous}\ L\ (\text{constant}). \quad (11)$$

Conversely, if a rock mass is well-described by LaModel, an equivalent overburden mass model should vary elastic modulus to keep the product of modulus and panel width constant. This relationship underscores how much the laminated overburden model departs from the homogeneous elastic body often employed in volume element and other boundary element methods.

LaModel uses only a fraction of the parameters defined for the volume element model since fundamental assumptions limit the range of material behavior. For instance, roof interfaces have no strength, and the layers are elastic and cannot fail. Abutment and pillar yielding are defined by the empirical Mark-Bieniawski equation [33] applied to pillars. This both simplifies and limits this approach. Simplification speeds model development and execution. However, the user must understand how this limits the range of behavior that can be modeled.

Overburden properties are defined in LaModel for a set of strata layers of uniform thickness separated by frictionless interfaces. All of the strata beams have the same properties. Thus, overall properties equivalent to the generic model layers have to be estimated. This was attempted in two ways – by finding an equivalent bending stiffness and by finding a weighted average for a given layer thickness. In the equivalent bending stiffness method, each member of the roof column was treated as a cantilever and sufficient force was applied at the end of the cantilever to achieve one unit of displacement. The required forces were combined and used in the cantilever displacement equation [39] to determine an equivalent Young's modulus. Second, a weighted average was found, weighted according to member height. A range of layer properties and interval thicknesses were tested (summarized in table 2). Gob stress-closure was modeled using equations by Zipf [47] and Heasley [16], with parameters fit to match the Salamon equation used in the FLAC model.

Table 2. LaModel overburden parameters.

Condition	Description
LaModel rock properties	Equivalent overburden to FLAC model determined with both equivalent stiffness and weighted thickness methods for each layer thickness.
LaModel layer interval	7.6, 15, 31, 61, 150, 305, and 610 m (25, 50, 100, 200, 500, 1000, 2000 ft)

MODEL RESULTS

Three key model results are (1) shifting of stress to panel abutments and gob, (2) distribution of stress in the abutment, and (3) deformation and failure of bridging strata. These results are compiled and compared with in-mine observations and the empirical model underlying ALPS and ARMPS.

(1) Shifting of Stress

The proportion of stress that shifts to abutments is a basic model result and has a large impact on other results. Figure 7 shows the range of proportion of the overpanel weight that is shifted to the abutment by modeling tool. The range of results for FLAC and LaModel includes all cases of shale and sandstone thickness described earlier for a panel width of 240 m (800 ft) and overburden thickness of 610 m (2000 ft). The ALPS column shows the range at this same overburden thickness for a range of β from 21° to 38.6°, the latter value from Allgaier [3], where 21° and 38.6° are located at the bottom and top, respectively of the indicated range. The volume-element results show very high transmission of stress to the abutment,

implying minimal loading of the gob. LaModel results show the largest range of results. Thinner layers increase roof flexibility and, thus, shift load from abutments to gob. The empirical method is consistent with thicker layers in the boundary element model while both fall slightly short of abutment loading calculated with the volume element method.

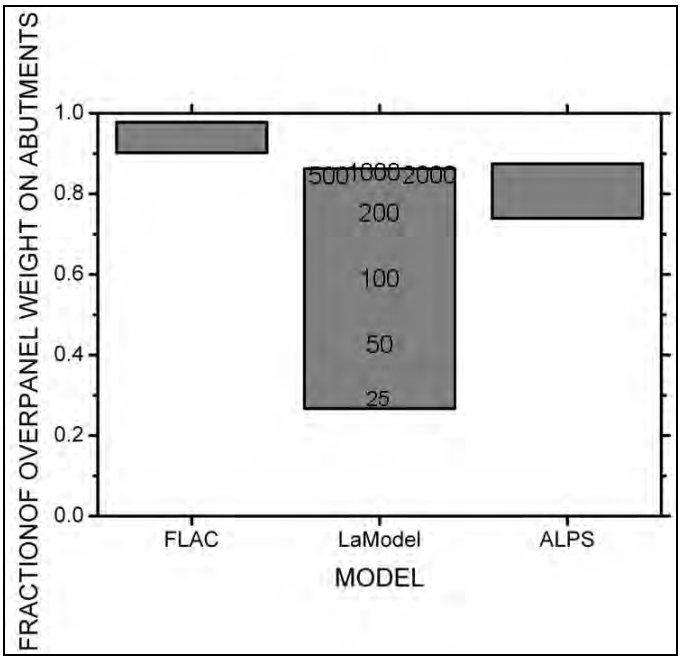

Figure 7. Chart showing the range of proportion of overpanel weight shifted to abutments for three modeling methods for a panel width of 240 m (800 ft) and an overburden thickness of 610 m (2000 ft). The locations of numbers in the LaModel column represent average result for that layer interval, where the interval is in ft.

(2) Abutment Stress Distribution

The distribution of stress shifted to the abutment is another important result. Stress shifted to the immediate rib can drive yielding and, possibly, outbursting of coal. Stress carried deeper in the abutment may impact neighboring excavations and is a particular concern for excavation of new entries, etc. Typical results are illustrated in figure 8. In the figure, overburden elastic properties were determined by the weighted thickness method. Results calculated with overburden properties determined by the equivalent stiffness method were similar and, therefore, not included in the figure. One of the most powerful FLAC results is the contrast between an immediate thick sandstone roof and a shale interval in the immediate roof. The shale limits peak stress in the coal and increases depth of yielding, moving stress away from the abutment rib. The assumed stress distribution used in the ALPS method predicts a much lower peak stress, but this peak is located at the ribline (recall figure 5).

The total area under the curve in an abutment stress plot is equivalent to the transferred load. Figure 7 shows that the stress transferred to the abutment should be greatest for the volume element model, and least for the most flexible boundary element cases. This is not evident in figure 8, largely because the right-hand "tail" of the curves has been truncated. In the truncated portions of the curves, the volume element and thick layer boundary element models have higher stress levels.

The distance that these models can transfer significant stress levels was characterized by the location at which the mining induced stress surcharge decayed to 50% of the overburden stress. The ranges of the 150% total stress level is plotted for a number of cases by method in figure 9, and the range of the 200% total stress level is similarly plotted in figure 10 for comparison. In these figures, the LaModel results with the smallest interface spacing plot at the bottom of the indicated range. LaModel results with interface spacing closer to overburden depth plot at the top of the indicated range.

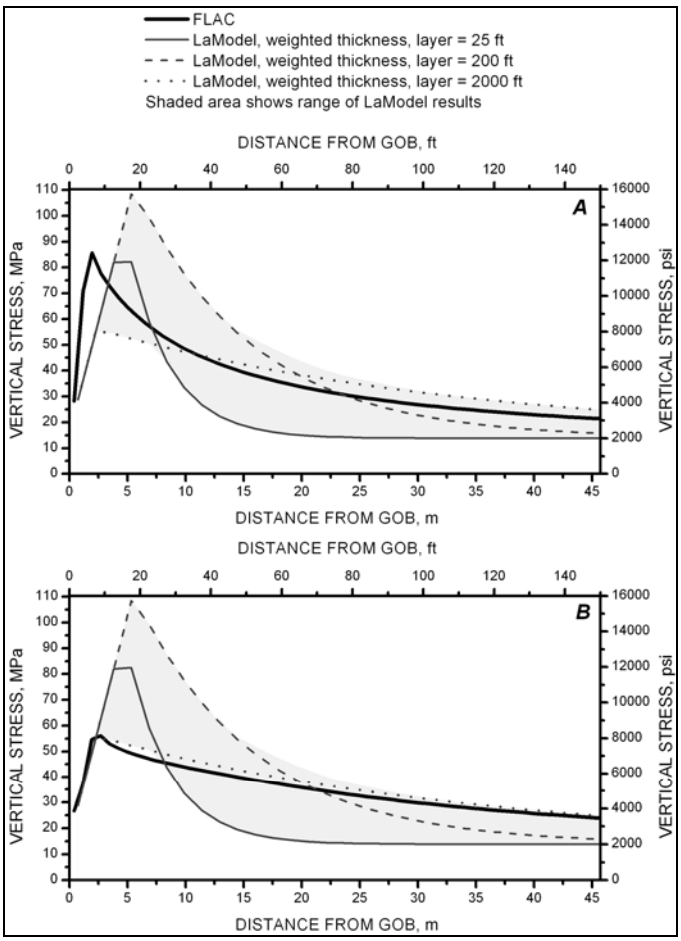

Figure 8. Vertical stress profile on abutment for the generic model case of 61 m (200 ft) of roof sandstone. Gob is modeled. A, No immediate roof shale; B, Immediate roof shale thickness is 15 m (50 ft).

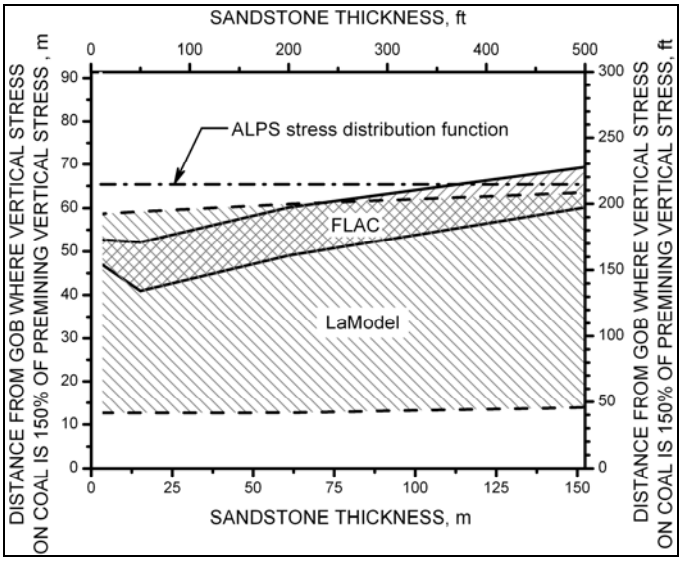

Figure 9. Distance from gob where vertical stress on coal is 150% of premining vertical stress. Results include immediate shale thickness of 0, 3.0, and 15 m (0, 10, and 50 ft) and all LaModel layer intervals modeled.

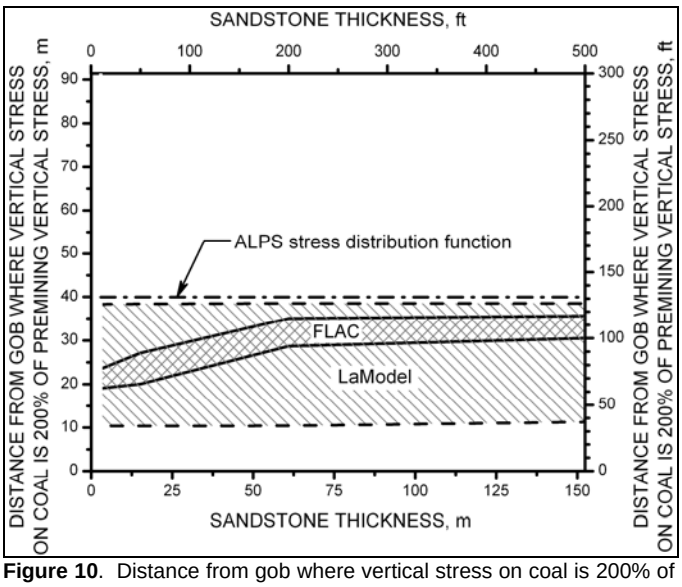

Figure 10. Distance from gob where vertical stress on coal is 200% of premining vertical stress. Results include immediate shale thickness of 0, 3.0, and 15 m (0, 10, and 50 ft) and all LaModel layer intervals modeled.

(3) Bridging Strata

The behavior of strata bridging or arching over the mined panel determines how much load is shifted to the abutments and influences how this load is carried within the strata. Overlying strata will also deform as they are undercut, a relationship often plotted as a ground reaction curve. In pillared panels, the slope or stiffness of this curve, in comparison to the post-peak curve of the pillar, determines whether one mode or mechanism of pillar bump occurs (figure 11). A ground reaction curve can be developed in FLAC or LaModel, but not from the empirical relationships described earlier.

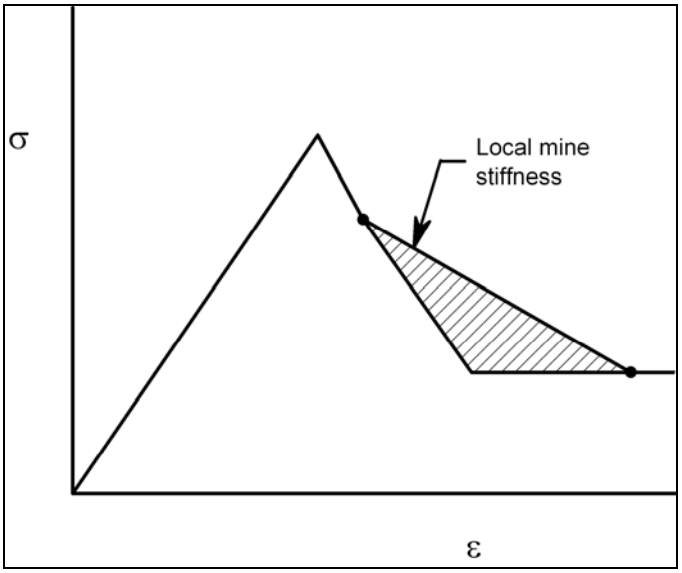

Figure 11. Post peak bump model comparing the descending slopes of a pillar with a flatter ground. reaction curve. The area of the shaded region represents the energy released kinetically (after Crouch and Fairhurst [10]).

Ground reaction curves have historically been determined by one of two methods. Starfield and Wawersik [44] used a perturbation method in which a strip or element is displaced or converged by a small specified amount. Equilibrium conditions are recalculated and the stress on the strip is determined. Local mine stiffness at that element is given by the decrease in stress per increase in compressive strain. In short, this method provides a single value for stiffness that corresponds to an infinitesimal closure of an entry or panel.

Salamon [41] replaced a pillar by a jack exerting the same forces, and then incrementally lowered pressure in the jack to create a ground reaction curve that may vary in stiffness as pressure is reduced. He then applied a rigorous mathematical approach to determine stability. In this study, we used the approach of a jack which incrementally reduces the applied pressure to the roof and floor of the gob. A variation of this method was used in LaModel. In these calculations, the Young's modulus of the gob elements was reduced in various stages to reduce stress transfer between the roof and floor. While this did not provide a uniform reduction of force, it did provide a nearly linear stiffness reduction that was close to the desired result.

Ground reaction curves were determined at mid-panel with FLAC and LaModel for the case of no immediate roof shale and 15 m (50 ft) of roof sandstone. In the case of FLAC, vertical stresses on the floor and roof of the cave were determined before excavation and stored in arrays. These stresses were applied in place of the excavated gob and then incrementally decreased. The model was allowed to come to equilibrium in each increment. Applied stress was then plotted against closure strain (figure 12).

In LaModel simulations, Young's modulus of the coal was incrementally reduced to simulate an incremental reduction of applied stress to the excavation roof and floor. When the layer interval was set low (for example, 7.6, 15 or 31 m [25, 50, or 100 ft]), it was possible for the closure to exceed seam height, at which point the curve was terminated.

Figure 12 shows examples of these ground reaction curves. The initial ground reaction curve stiffness calculated with FLAC is similar to that from LaModel for layer thicknesses of 150 m, 305 m, and 610 m (500 ft, 1000 ft, and 2000 ft). However, the FLAC model stiffness changes suddenly as stress is almost entirely removed, indicating strata collapse (the "elbow" in this curve in Figure 12). Such collapses can be an important failure mechanism where overburden includes strong strata (e.g., [7;45]). The corresponding state of failure calculated by FLAC for this case (no immediate roof shale and 15 m [50 ft] of roof sandstone) is shown in figure 13. The sandstone failed in tension, and the soft shale failed significantly, both in shear and tension along ubiquitous joints. In this case, the sandstone in the roof likely prevented caving completely to the surface. It is interesting to note that the angle of failure was 16° to 18°, similar to the average ALPS angle, β = 21°. In addition, the failure surfaces tended to break horizontally along the ubiquitous joints.

LaModel cannot follow this type of behavior since it is limited to elastic overburden behavior. Thus, it may be necessary to check for possible collapse when using LaModel. For example, Newman [36] verified his LaModel result by confirming that the maximum self-supporting span of a strata beam was greater than panel width.

MODEL EVALUATION

The most important conclusion that can be drawn is that the empirical, volume element and boundary element methods reviewed differ in the ranges of behavior that can be accessed. This is especially evident where failure of bridging overburden might occur. It also applies to any impact of horizontal stress which is not modeled by the LaModel program. The analyst must insure that all important behavior modes are considered, although this consideration may make use of a variety of calculations and models.

A second conclusion is that a comparison to real ground behavior is needed to focus the modeling effort. In this study, a wide range of results were produced from small variations within a simple site model and choice of analysis method. Ground behavior information can include observations, like reports of long stress transfer distance, or direct measurements. Quantitative data might include pressure measurements made in the gob or abutment. Gob measurements are relatively rare. Those that have been made indicate that gob can carry significant loads [8;26], particularly where vertical joints are frequent

[26]. Of course, vertical joints were not explicitly considered by any of the models considered here. Thus, their contribution can only be accounted for by "calibrating" models.

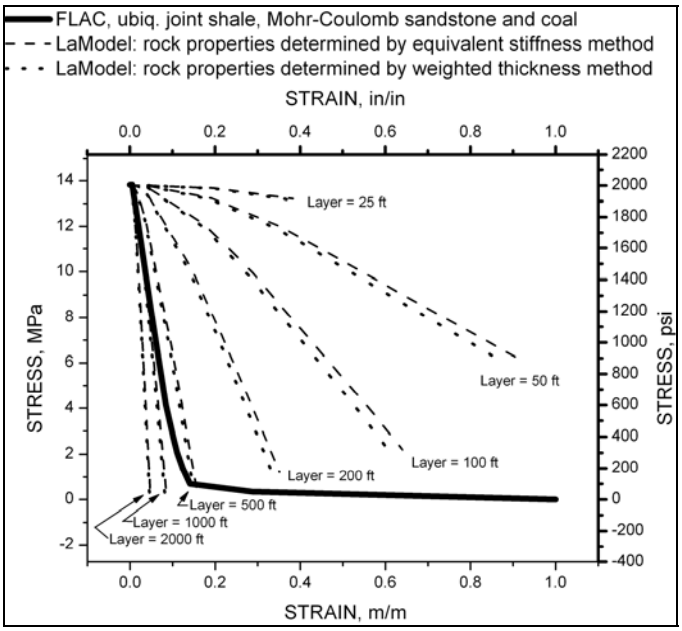

Figure 12. Ground reaction curves at mid-panel for cases of no immediate roof shale and roof sandstone thickness = 15 m (50 ft).

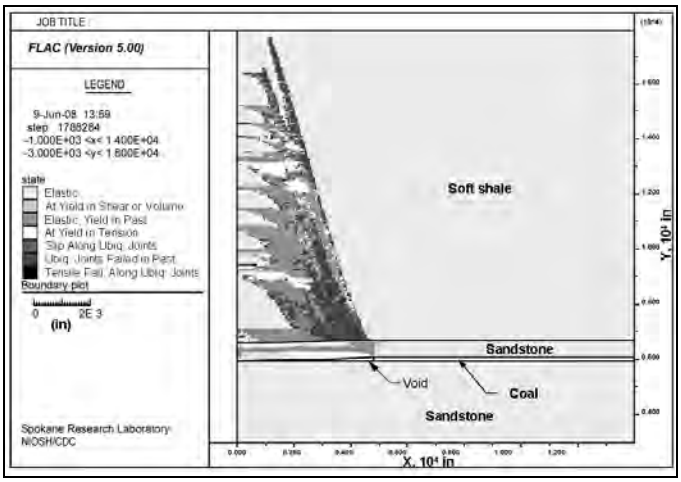

Figure 13. State of zones in FLAC model showing failure of sandstone and soft shale for case of Mohr-Coulomb sandstone (15 m [50 ft]) and coal (1.5 m [10-ft]), and complete excavation of coal. The legend indicates whether a zone is elastic, has yielded or failed, has yielded or failed in the past but is currently elastic, and kind of yield or failure. This view does not show the entire model.

Borehole pressure cell measurements in pillars and abutments are easier to make and are somewhat more plentiful. A calibration is demonstrated for two such cases from the literature in figures 14 and 15 [5;24]. These cases contain gate road entries not included in the models. However, aside from local perturbations around entries, each can be optimized to provide the best possible approximation of the measured stress distribution. In this case, the quality of fit increases with complexity from empirical, to boundary element, to volume element, which is hardly surprising. The choice of model and model parameters would follow based on closeness of fit and the relative effort required by alternative methods.

A third conclusion is that, for this generic site model, there is no "equivalent" LaModel boundary element model that follows easily from a volume element model with a strong stratum. This conclusion arises from strong differences in the way overburden is modeled by these methods. One reflection of this difference, is that the product of lamination thickness and modulus, not the modulus itself, is a key input to LaModel. Note that for each calibration case in figures 14 and 15, two LaModel runs with variations of overburden modulus and lamination thickness that satisfy equation (9) have identical plots. As such, the default layer thickness of 50 ft can be used for all models, provided appropriate adjustments are made to overburden modulus. This may, however, result in a modulus that departs markedly from a realistic range of properties as determined by other methods.

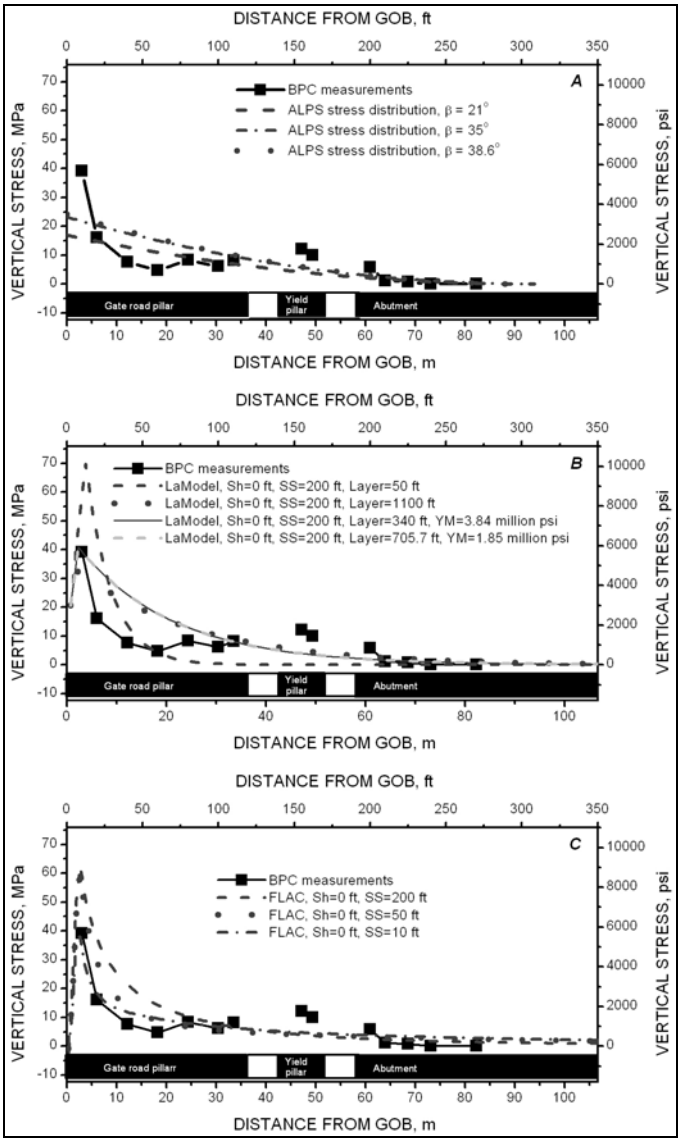

Figure 14. Mining-induced stress around the 6th Right gate roads at a Utah Mine [24]. A, ALPS assumed stress distribution function and measurements; B, LaModel results, including calibrated models with measurements; and C, FLAC results with measurements.

DISCUSSION AND CONCLUSIONS

Empirical, boundary element, and volume element modeling programs are often used in assessing the performance of mine plans. The selection of a modeling tool is important and essential in the modeling process. Making the right choice depends on understanding the relative merits of these tools and their abilities to simulate ground response to mining in the context of a particular site – in this case, a generic site model typical of deep western coal mines. The most remarkable element of this model is inclusion of an interval of strong, bridging strata.

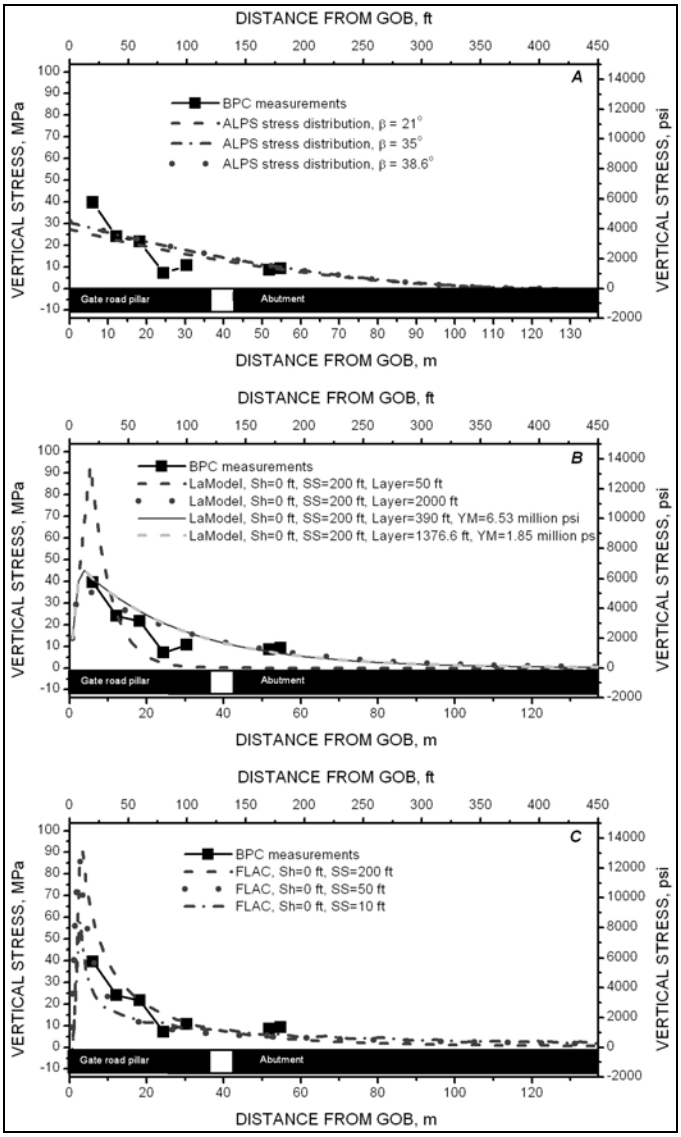

Figure 15. Mining-induced stress around the 9th East gate roads at a Utah Mine [5]. A, ALPS assumed stress distribution function and measurements; B, LaModel results, including calibrated models with measurements; and C, FLAC results with measurements.

The most important consideration is whether a design project considers all possible modes of ground response to mining. For empirical methods, this concern is best addressed by comparing conditions at underlying cases with those for the application. A mismatch may compromise empirical method results. It is also important to recognize and, if necessary, compensate for the fact that the boundary element program, LaModel, does not consider the effects of horizontal stresses and failure of the overburden.

This work also showed that the assumptions and features of these volume and boundary element programs differ too markedly for a model constructed in one to be "converted" into the other through application of the same input parameters. Thus, care must be taken when taking input parameters from past analyses using different modeling programs. New models should be calibrated to field observations and, ideally, measurements of critical behavior.

Finally, for the site model considered here, the degree of sophistication correlated well with ability to match borehole pressure cell measurements at a typical site. This is not necessarily a general result, but is consistent with the greater level of detail available in volume element models. The fidelity required of a model is necessarily constrained by uncertainty in input and calibration measurements. However, it is essential that all significant ground behaviors, especially failure modes, are considered in the course of a design project. Ignoring a possible failure mechanism simply because it is ruled out by a program's underlying assumptions is not acceptable practice. At the same time, the level of effort required to achieve desired detail with a volume-element model may require much larger preparation and computation times, possibly making this approach impractical or, in some cases, practically impossible. FLAC models described here took up to 14 days to solve with a modern workstation. In such cases, application of a variety of simpler models and calculations addressing various aspects of panel behavior may be advantageous.

ACKNOWLEDGMENTS

The authors would like to thank Dr. Keith Heasley for discussions that strengthened this paper.

REFERENCES

1. Agapito, J. F. T., R. R. Goodrich, and M. Moon (1997) Dealing with Coal Bursts at Deer Creek. *Mining Engineering,* Vol. 49, No. 7, pp. 31-37.

2. Agapito, Joe F. T. and Rex R. Goodrich (2000) Five Stress Factors Conducive to Bumps in Utah, USA, Coal Mines. In *Proceedings: 19th International Conference on Ground Control in Mining*, Peng, Syd S. and Christopher Mark (eds.) (Morgantown, WV, August 8-10, 2000) Morgantown, WV: West Virginia University, pp. 93-100.

3. Allgaier, Frederick K. (1988) Surface Subsidence Over Longwall Panels in the Western United States—Final Results at the Deer Creek Mine, Utah. U.S. Bureau of Mines, Bureau of Mines Information Circular 9194, 21 pp.

4. Badr, S., U. Ozbay, S. Kieffer, and M. Salamon (2003) Three-Dimensional Strain Softening Modeling of Deep Longwall Coal Mine Layouts. In *FLAC and Numerical Modeling in Geomechanics*, Brummer, et al. (eds.) Lisse: Swets & Zeitlinger, pp. 233-239.

5. Barron, Lance R. (1990) Longwall Stability Analysis of a Deep, Bump-Prone Western Coal Mine—Case Study. In *Proceedings: 9th International Conference on Ground Control in Mining*, Peng, Syd S. (ed.) (Morgantown, WV, June 4-6, 1990) Morgantown, WV: University of West Virginia, pp. 142-149.

6. Beer, Ferdinand P. and E. Russel Johnston, Jr. (1981) *Mechanics of Materials*. New York: McGraw-Hill Book Company, 634 pp.

7. Board, M., B. Damjanac, and M. Pierce (2007) Development of a Methodology for Analysis of Instability in Room and Pillar Mines. In *Deep Mine 07, Proceedings of the Fourth International Seminar on Deep and High Stress Mining*, Potvin, Y. (ed.) (Perth, Australia, November 7-9, 2007) Perth: Australian Centre for Geomechanics, pp. 273-282.

8. Campoli, Alan A., Timothy M. Barton, Fred C. Van Dyke, and Gauna Michael (1993) Gob and Gate Road Reaction to Longwall Mining in Bump-Prone Strata. U.S Department of the Interior, Bureau of Mines Report of Investigations 9445, 56 pp

9. Chen, J., M. Mishra, and J. DeMichiei (1999) Design Considerations for Bump-Prone Longwall Mines. In *Proceedings: 18th Conference on Ground Control in Mining*, Peng, Syd S. and Christopher Mark (eds.) (Morgantown, WV, August 3-5, 1999) Morgantown, WV: West Virginia University, pp. 124-135.

10. Crouch, S. L.and C. Fairhurst (1974) Mechanics of Coal Mine Bumps. *Transactions,* Vol. 256, pp. 317-323.

11. DeMarco, Matthew J., J. R. Koehler, and Hamid Maleki (1995) Gate Road Design Considerations for Mitigation of Coal Bumps in Western U.S. Longwall Operations. In *Proceedings: Mechanics*

and Mitigation of Violent Failure in Coal and Hard-Rock Mines, Maleki, Hamid, Priscilla F. Wopat, Richard C. Repsher, and Robert J. Tuchman (eds.) Bureau of Mines Special Publication 01-95, U.S. Department of the Interior, pp.141-165.

12. Gilbride, Leo J. and Michael P. Hardy (2004) Interpanel Barriers for Deep Western U.S. Longwall Mining. In *Proceedings: 23rd International Conference on Ground Control in Mining*, Peng, Syd S., Christopher Mark, Gerry Finfinger, Steve Tadolini, A. Wahab Khair, and Keith Heasley (eds.) (Morgantown, WV, August 3-5, 2004) Morgantown, WV: University of West Virginia, pp. 35-41.

13. Goodrich, R. R., J. F. T. Agapito, C. Pollastro, L. LaFrentz, and K. Fleck (1999) Long Load Transfer Distances at the Deer Creek Mine. In *Rock Mechanics for Industry, Proceedings of the 37th U.S. Rock Mechanics Symposium*, Amadei, Bernard, Robert L. Kranz, Gregg A. Scott, and Peter H. Smeallie (eds.) (Vail, Colorado, June 6-9, 1999) Rotterdam: A.A. Balkema, pp. 517-523.

14. Haramy, K. Y., J. A. Magers, and J. P. McDonnell (1988) Mining Under Strong Roof. In *Proceedings: 7th International Conference on Ground Control in Mining*, Peng, Syd S. (ed.) (Morgantown, WV, August 3-5, 1988) Morgantown, WV: West Virginia University, pp. 179-194.

15. Heasley, Keith A. (1998) *Numerical Modeling of Coal Mines with a Laminated Displacement-Discontinuity Code.* Ph.D. Dissertation. Colorado School of Mines, 187 pp.

16. Heasley, Keith A. (2007) LAMODEL ver. 2.1. West Virginia University.

17. Heasley, Keith A. (2008) Back Analysis of the Crandall Canyon Mine Using the LaModel Program. Appendix S in *Mine Safety and Health Administration, Report of Investigation, Underground Coal Mine, Fatal Underground Coal Burst Accidents, August 6 and 16, 2007, Crandall Canyon Mine*, CAI-2007-15-17.19-24, Arlington, VA: U.S. Department of Labor, 51 pp.

18. Heasley, Keith A. (2008) Some Thoughts on Calibrating LaModel. In *Proceedings: 27th International Conference on Ground Control in Mining*, Peng, Syd S., Christopher Mark, Gerry Finfinger, Steve Tadolini, A. Wahab Khair, Keith A. Heasley, and Yi Luo (eds.) (Morgantown, WV, July 29-31, 2008) Morgantown, WV: West Virginia University, pp. 7-13.

19. Holland, Charles T. (1963) Pressure Arch Techniques. *Mechanization—The Business Magazine for Coal Mining,* Vol. 27, No. 3, pp. 45-48.

20. Itasca Consulting Group, Inc. (2006) *FLAC : Fast Lagrangian Analysis of Continua — User's Guide.*

21. Jones, R. E. , W. G. Pariseau, V. Payne, and G. Takenaka (1990) Sandstone Escarpment Stability in Vicinity of Longwall Mining Operations. In *Rock Mechanics Contributions and Challenges: Proceedings of the 31st U.S. Symposium*, Hustrulid, W. A. and G. A. Johnson (eds.) (Colorado School of Mines, June 18-20, 1990) Rotterdam: A. A. Balkema, pp. 555-562.

22. Kelly, M. (1999) 3D Aspects of Longwall Geomechanics. In *Ground Behaviour and Longwall Faces and its Effect on Mining, Exploration and Mining*, Report 560F, ACARP Project C5017, 28 pp.

23. Koehler, J. R. (1994) The History of Gate Road Performance at the Sunnyside Mines: Summary of U.S. Bureau of Mines Field Notes. U.S. Department of the Interior, Bureau of Mines Information Circular 9393, 43 pp.

24. Koehler, J. R., M. J. DeMarco, R. J. Marshall, and J. Fielder (1996) Performance Evaluation of a Cable Bolted Yield-Abutment Gate Road System at the Crandall Canyon No. 1 Mine, Genwall Resources, Inc., Huntington, Utah. In *Proceedings: 15th International Conference on Ground Control in Mining*, Ozdemir, Levent, Kanaan Hanna, Khamis Y. Haramy, and Syd Peng (eds.) (Golden, Colorado, August 13-15, 1996) Golden, Colorado: Colorado School of Mines, pp. 477-495.

25. Maleki, H. (1995) An Analysis of Violent Failure in U.S. Coal Mines—Case Studies. In *Proceedings: Mechanics and Mitigation of Violent Failure in Coal and Hard-Rock Mines*, Maleki, Hamid, Priscilla Wopat, Richard C. Repsher, and Robert J. Tuchman (eds.) Special Publication 01-95, U.S. Department of the Interior, pp. 5-25.

26. Maleki, H., W. Hustrulid, and D. Johnson (1984) Pressure Measurements in the Gob. In *25th U.S. Symposium on Rock Mechanics*, (Evanson, Illinois) pp. 533-545.

27. Maleki, H. N., J. F. T. Agapito, and M. Moon (1988) In-Situ Pillar Strength Determination for Two-Entry Longwall Gates. In *Proceedings: 7th International Conference on Ground Control in Mining*, Peng, Syd S. (ed.) (Morgantown, WV, August 3-5, 1988) Morgantown, WV: West Virginia University, pp. 10-19.

28. Maleki, Hamid (1988) Ground Response to Longwall Mining: A Case Study of Two-Entry Yield Pillar Evolution in Weak Rock. *Colorado School of Mines Quarterly,* Vol. 83, No. 3, 60 pp.

29. Maleki, Hamid (2006) Caving, Load Transfer, and Mine Design in Western U.S. Mines. In *Golden Rocks 2006, The 41st U.S. Symposium on Rock Mechanics (USRMS): "50 Years of Rock Mechanics — Landmarks and Future Challenges"*, Yale, David, Sarah Holtz, Chris Breeds, and Ugur Ozbay (eds.) (Golden, Colorado, June 17-21, 2006) Paper 06-931, 10 pp.

30. Maleki, Hamid (2008) The In-Situ Pillar Strength and Overburden Stability in U.S. Mines. In *Proceedings: 27th International Conference on Ground Control in Mining*, Peng, Syd S., Christopher Mark, A. Wahab Khair, and Keith A. Heasley (eds.) (Morgantown, WV, July 29-31, 2008) Morgantown, WV: West Virginia University, pp. 60-65.

31. Mark, Christopher (1987) *Analysis of Longwall Pillar Stability .* Ph.D. Thesis. The Pennsylvania State University, 443 pp.

32. Mark, Christopher (1990) Pillar Design Methods for Longwall Mining. U.S. Bureau of Mines Information Circular 9447, 55 pp.

33. Mark, Christopher and Frank E. Chase (1997) Analysis of Retreat Mining Pillar Stability (ARMPS). In *Proceedings: New Technology for Ground Control in Retreat Mining*, Mark, Christopher and Robert J. Tuchman (eds.) Information Circular 9446, NIOSH, pp. 17-34.

34. Mine Safety and Health Administration (2008) Rock Mass Properties. Appendix V in *Mine Safety and Health Administration, Report of Investigation, Underground Coal Mine, Fatal Underground Coal Burst Accidents, August 6 and 16, 2007, Crandall Canyon Mine*, ID No. 42-01715, Arlington, VA: Department of Labor, Mine Safety and Health Administration,

35. National Coal Board, Production Department (1975) *Subsidence Engineers' Handbook*. London: National Coal Board, 111 pp.

36. Newman, David (2008) Coal Mine Bumps: Case Histories of Analysis and Avoidance. In *Proceedings: 27th International Conference on Ground Control in Mining*, Peng, Syd S. , Christopher Mark, Gerry Finfinger, Steve Tadolini, A. Wahab Khair, Keith A. Heasley, and Yi Luo (eds.) (Morgantown, WV, July 29-31, 2008) Morgantown, WV: West Virginia University, pp. 1-6.

37. Pappas, Deno M. and Christopher Mark (1993) Behavior of Simulated Longwall Gob Material. U.S. Department of the Interior, Bureau of Mines Report of Investigations 9458, 42 pp.

38. Pariseau, William G. (2007) Finite Element Analysis of Inter-Panel Barrier Pillar Width at the Aberdeen (Tower) Mine. August 30, 2007, 50 pp.

39. Parker, Harry (1975) *Simplified Engineering for Architects and Builders*, Fifth edition. New York: John Wiley & Sons, p. 60, 435 pp.

40. Peng, Syd S. and H. S. Chiang (1984) *Longwall Mining*. New York: John Wiley & Sons, 720 pp.

41. Salamon, M. D. G. (1970) Stability, Instability and Design of Pillar Workings. *Int. J. Rock Mech. Min. Sci.,* Vol. 7, No. 1, pp. 613-631.

42. Salamon, M. D. G. (1990) Mechanism of Caving in Longwall Coal Mining. In *Rock Mechanics Contributions and Challenges: Proceedings of the 31st U.S. Symposium*, Hustrulid, W. A. and G. A. Johnson (eds.) (Golden, Colorado, June 18-20, 1990) A.A. Balkema, pp. 161-168.

43. Sinha, K. P. (1979) *Displacement Discontinuity technique for analyzing stress and displacements due to mining in seam deposits.* Ph.D. Thesis. University of Minnesota, 311 pp.

44. Starfield, A. M. and W. R. Wawersik (1968) Pillars as Structural Components in Room-and-Pillar Mine Design. In *Basic and Applied Rock Mechanics, Proceedings: Tenth Symposium on Rock Mechanics*, Gray, Kenneth E. (ed.) (Austin, Texas, May 20-22, 1968) New York: Society of Mining Engineers of AIME, pp. 793-809.

45. Whyatt, Jeff and Floyd Varley (2008) Catastrophic Failures of Underground Evaporite Mines. In *Proceedings: 27th International Conference on Ground Control in Mining*, Peng, Syd S., Christopher Mark, Gerry Finfinger, Steve Tadolini, A. Wahab Khair, Keith Heasley, and Yi Luo (eds.) (Morgantown, WV, July 29-31, 2008) Morgantown, WV: West Virginia University, pp. 113-122.

46. Zipf, R. Karl, Jr. (1992) MULSIM/NL Application and Practitioner's Manual. USBM Information Circular 9322, 44 pp.

47. Zipf, R. Karl, Jr. (1992) MULSIM/NL Theoretical and Programmer's Manual. USBM Information Circular 9321, 52 pp.

APPENDIX

Table 1. Estimated properties of materials as used in the generic model.

Property	Soft shale	Sandstone	Shale	Coal
Young's modulus, GPa	10.3	34.6	13.8	3.45
Young's modulus, psi	1.50 million	5.00 million	2.00 million	0.50 million
Poisson's ratio	0.35	0.25	0.35	0.30
Density, kg/m^3	2310	2310	2310	1280
Density, lb/ft^3	144	144	144	80
Cohesion, MPa	20.5	33.8	20.5	7.09
Cohesion, psi	2970	4910	2970	1030
Friction angle	30°	25°	30°	30°
Dilation angle	5°	5°	5°	5°
Tensile strength, MPa	2.07	5.03	6.89	2.07
Tensile strength, psi	300	730	1000	300
Ubiquitous joint angle	0°	--	0°	--
Ubiquitous joint cohesion, MPa	1.4	--	1.4	--
Ubiquitous joint cohesion, psi	200	--	200	--
Ubiquitous joint friction angle	25°	--	25°	--
Ubiquitous joint dilation angle	5°	--	5°	--
Ubiquitous joint tensile strength, MPa	0.83	--	0.83	--
Ubiquitous joint tensile strength, psi	120	--	120	--